HHS Public Access

Author manuscript

Reprod Toxicol. Author manuscript; available in PMC 2018 June 01.

Published in final edited form as:

Reprod Toxicol. 2017 June ; 70: 60–69. doi:10.1016/j.reprotox.2016.11.005.

Identification of vascular disruptor compounds by analysis in zebrafish embryos and mouse embryonic endothelial cells

Catherine W. McCollum[1,#], **Javier Conde Vancells**[2,#], **Charu Hans**[3], **Mercedes Vazquez-Chantada**[2], **Nicole Kleinstreuer**[4], **Tamara Tal**[5], **Thomas Knudsen**[6], **Shishir S. Shah**[3], **Fatima A. Merchant**[3,7], **Richard H. Finnell**[2], **Jan-Åke Gustafsson**[1,8], **Robert Cabrera**[2], and **Maria Bondesson**[1,9,*]

[1]Department of Biology and Biochemistry, Center for Nuclear Receptors and Cell Signaling, University of Houston, Houston 77204, TX, USA

[2]Department of Nutritional Sciences, Dell Pediatric Research Institute, The University of Texas at Austin, Austin 78723, TX, USA

[3]Department of Computer Science, University of Houston, Houston 77204, TX, USA

[4]NIEHS/DNTP/NICEATM, RTP 27560, NC, USA

[5]U.S. EPA/ORD/ISTD, RTP 27711, NC, USA

[6]U.S. EPA/ORD/NCCT RTP 27711, NC, USA

[7]Department of Engineering Technology, University of Houston, Houston 77204, TX, USA

[8]Department of Biosciences and Nutrition, Novum, Karolinska Institutet, 141 83 Stockholm, Sweden

[9]Department of Pharmacological and Pharmaceutical Sciences, University of Houston, Houston 77204, TX, USA

Abstract

To identify vascular disruptor compounds (VDCs), this study utilized an *in vivo* zebrafish embryo vascular model in conjunction with a mouse endothelial cell model to screen a subset of the U.S. Environmental Protection Agency (EPA) ToxCast Phase I chemical inventory. In zebrafish, 161 compounds were screened and 34 were identified by visual inspection as VDCs, of which 28 were confirmed as VDCs by quantitative image analysis. Testing of the zebrafish VDCs for their

[*]Corresponding author: Maria Bondesson, University of Houston, Department of Pharmacological and Pharmaceutical Sciences, 3605 Cullen Blvd, Science and Engineering Research Center Bldg. 545, Houston, TX 77204, Phone: 832-842-8805, mbondessonbolin@uh.edu.

[#]Equal contribution

Conflict of interest: We declare no conflict of interest.

capacity to inhibit endothelial tube formation in the murine yolk-sac-derived endothelial cell line C166 identified 22 compounds that both disrupted zebrafish vascular development and murine endothelial *in vitro* tubulogenesis. Putative molecular targets for the VDCs were predicted using EPA's Toxicological Prioritization Index tool and a VDC signature based on a proposed adverse outcome pathway for developmental vascular toxicity. In conclusion, our screening approach identified 22 novel VDCs, some of which were active at nanomolar concentrations

Keywords

zebrafish; mouse endothelial cells; angiogenesis; vascular development; vascular disruptor compounds

Introduction

There is mounting concern and evidence for adverse human health effects due to elevated exposure to environmental pollutants in the forms of pesticides and industrial chemicals [1–4]. One of the toxicity endpoints relevant for human health is disruption of vascular development [5]. The vascular network is the first fully functional tissue system to be formed during embryonic development. Consequently, vascular structural and functional defects can be deleterious for the fetus resulting in multi-organ system anomalies [6]. For example, prenatal exposure to thalidomide, a drug prescribed to pregnant women in the 1950s and 60s for nausea and morning sickness, has been shown to be teratogenic on limb development (phocomelia) following disruption of the immature vascular network [7]. Other human health effects of vascular disruption have been described in human cohort studies, such as demonstrating that exposure to environmental arsenic leads to perturbed placental angiogenesis, which is linked to reduced birth weight [8–10].

The importance of normal vascular development for reproduction has been shown in genetically modified mice with gene inactivation of *Vegfr1* and 2, *Arnt* and *Hif1a/Hif2a*, among other genes [11–13]. In these mice, early embryonic vascular development and placental angiogenesis are perturbed, the latter leading to failed implantation of the embryos. In addition to genetic status, exposure to certain environmental chemicals adversely affects vascular development of the fetus. Compounds that have vascular disruption activity *in vivo* include BPA and permethrin in mice [14, 15] and arsenic, cartap, TCCD, and cadmium in zebrafish ([16, 17] and reviewed in McCollum [18]). However, the vast majority of environmental chemicals have not been analyzed for vascular disruption activity, partly due to the lack of complex, mechanistically driven or *in vivo* high throughput screening (HTS) models.

Zebrafish have been extensively used as genetic and embryonic models for vascular development [19, 20]. Transgenic fish expressing fluorescence in endothelial cells provide an approach to evaluate vascular development in an integrative whole-animal model. Vascular tissues develop through two processes: vasculogenesis and angiogenesis. In zebrafish, vasculogenesis starts with angioblasts arising in the ventrolateral mesoderm to form the axial vessel primordial [21, 22] . Endothelial cells (ECs), developmentally derived from these angioblasts, migrate and coalesce at the midline to differentiate into the dorsal

aorta (DA) and posterior cardinal vein (PCV). Subsequently, during angiogenesis, endothelial cells sprout, migrate and proliferate to assemble the final vascular network. At approximately 20 hours post fertilization (hpf), primary intersegmental vessels (ISVs) sprout bilaterally from the DA and extend dorsally towards the dorsolateral roof of the neural plate and form the dorsal longitudinal anastomotic vessel (DLAV) [23]. The zebrafish caudal vein plexus (CVP) is formed by venous-specific angiogenesis at approximately 25 hpf during which ECs sprout from the PCV and migrate ventrally to form a primordial plexus [24, 25]. By 48 hpf, the complex zebrafish CVP network is established. Although the vascular patterning is established by 72 hpf, the embryo with genetically or chemically perturbed blood vessels or circulation can survive several more days presumably due to oxygen diffusion through the skin [26, 27]. This trait provides a unique window of opportunity, in which vascular disruption can be studied prior to any potential effects on embryo viability.

The process of blood vessel development can be recapitulated *in vitro* using endothelial cells that form capillary-like structures (tubes) on a basement membrane matrix [28]. This *in vitro* system has been extensively exploited as a model to test whether chemicals have the ability to block or enhance angiogenesis. Human umbilical vein endothelial cells (HUVEC) are typically used in the tube formation assay. However, other cell lines with endothelial characteristics have also been utilized [29, 30], such as the endothelial cell line, C166, which is derived from the yolk sac of a transgenic Day 12 mouse embryo [31]. C166 cells assemble into capillary-like networks when placed on Matrigel, a basement membrane matrix secreted by Engelbreth-Holm-Swarm (EHS) mouse sarcoma cells [32]. Moreover, the cells retain a cobblestone-like morphology at confluence and express several markers of endothelial cells, such as angiotensin converting enzyme, scavenger receptors and VCAM-1. This *in vitro* system could be used to identify chemicals that disrupt vascular development.

Previously, chemicals from the ToxCast Phase I chemical library were ranked by their potential to be putative vascular disruptor compounds (pVDCs), based on bioactivity patterns across *in vitro* HTS assays for key molecular targets in vascular developmental signaling [33].

Furthermore, positive correlations were found between the highest ranking pVDCs and developmental defects in rats and rabbits from ToxRefDB (http://www.epa.gov/ncct/toxrefdb/), and an Adverse Outcome Pathway (AOP) for embryonic vascular disruption leading to adverse prenatal outcomes was proposed [5, 34].

The work presented here compared and expanded the identification of pVDCs from *in vitro* HTS assays and computational modeling by using functional angiogenesis assays in zebrafish embryos and mouse embryonic endothelial cells. We screened 161 chemicals from the ToxCast phase I library and used advanced image analysis to quantify the biological effects observed and rank the compounds. We also compared our VDC screening results to the chemicals' pVDC signatures determined from the ToxCast computational toxicology approach. Putative molecular targets were identified from pVDC signatures comprising of 124 HTS assays, spanning a wide range of biology relevant to angiogenesis including VEGFR-dependent signaling, vessel remodeling, extracellular matrix and chemokine signaling pathways [5, 33, 34] (Tal et al. RTX submitted manuscript to this issue 2016). We

propose that complementary models such as those in the present study can be used to prioritize chemicals for testing of vascular disruption in higher order vertebrates.

Materials and Methods

Fish husbandry

Zebrafish (*Danio rerio*) were reared and maintained at 28.5 °C as previously described [35], and in accordance with protocols approved by the Institutional Animal Care and Use Committee at University of Houston. A stable line of *Tg(kdrl:EGFP)mitfa*$^{b692/b692}$ was generated by crossing *Tg(kdrl:EGFP)* with *mitfa*$^{b692/b692}$ (Zebrafish International Resource Center, Eugene, OR) to facilitate GFP visualization without obstruction from melanophores. Embryos were collected from natural mating and staged accordingly [36].

Chemicals

All 161 chemicals were from ToxCast phase I chemical library (http://www.epa.gov/ncct/toxcast/chemicals.html). The chemicals were provided as stock library plates (96-well) from the National Center for Computational Toxicology, typically at 20mM concentration in dimethyl sulfoxide (DMSO). We first analyzed the top 50 chemicals (by pVDC score) listed in [33] followed by 111 chemicals picked in ascending order (starting with well #A1, A2, A3, and so on) from the stock plates of the ToxCast phase I library from EPA. Supplementary Table S1 lists the chemicals tested.

Zebrafish chemical treatments

Tg(kdrl:EGFP)^{mitfab692} fertilized eggs were harvested in a petri dish after mating. At approximately 3 hpf, embryos were sorted and placed in 6-well plates (n = 20/well), followed by a single chemical treatment without renewal at 100 nM, 250 nM, 500 nM, 1 μM, 10 μM or 20 μM, unless otherwise noted (Supplementary Table S1). If the chemical exposures were lethal, lower and narrower concentrations were tested. The final concentration of the vehicle was 0.1% DMSO. Each well contained a final volume of 3 ml of embryo medium, E3 (5 mM NaCl, 0.17 mM KCl, 0.33 mM $CaCl_2$, 0.33 mM $MgSO_4$). Control embryos were treated with vehicle (0.1% DMSO) alone. The embryos were incubated at 28.5 °C until 72 hpf, at which point they were evaluated for vascular perturbations.

Mouse C166 cell culture and tube formation assay

C166 cells were grown in Dulbecco's modified eagle medium (DMEM) supplemented with 10% fetal bovine serum (FBS) and 50 U/ml of penicillin-streptomycin. For chemical testing, cells were detached with trypsin-EDTA (0.25%) and resuspended in EGM-2 Bulletkit (Lonza, Walkersville, MD). Detached cells were counted in the hemocytometer and resuspended at a concentration of 230 cell/μl. Leaving the outer wells empty, 130 μl of the cell solution were dispensed in each well of a 96-well plate pre-coated with a thick (50 μl) layer of Matrigel (BD Biosciences, San Jose, CA). Serial dilutions of the 34 chemicals identified as positive in the zebrafish assay were immediately dispensed in the wells and the cells were incubated at 37°C in a humidified atmosphere containing 5% CO_2 and air for 150 minutes. C166 cells were treated in triplicate at 80 nM, 310 nM, 1.25 μM, 5 μM, and 20 μM

of each test chemical or vehicle alone with a final concentration of 0.1% DMSO. Each well contained a final volume of 200 μl.

Fluorescence and Cellular Imaging

At 72 hpf, control and treated embryos were manually dechorionated, if necessary, and anesthetized with 0.04% MS-222 (Pentair Aquatic Eco-Systems, Apopka, FL). Embryos were manually oriented and imaged laterally using a 4X objective on an Olympus IX51 fluorescence microscope equipped with an Olympus XM10 camera and cellSens Dimension software (Olympus, Center Valley, PA). The embryos were visually examined for vascular perturbations either in the GFP-expressing vasculature by fluorescence microscopy or for other vascular related effects by light microscopy. The vascular perturbations included perturbed ISVs (thin, short or non-overlapping ISVs from the left and right side), fewer vessels in any part of the body, abnormal DA or caudal vein (CV), uncondensed CVP, hemorrhages, thrombosis or pericardial edema. A chemical was classified as a VDC if 10% or more of the tested embryo population had a vascular perturbation, because occasionally a vascular perturbation was identified in untreated embryos (less than 10%).

Mouse C166 cells were imaged with an EVOS FL Base microscope system (Electron Microscopy Sciences, Hatfield, PA) at 4X magnification in phase contrast mode. Experiments were performed in triplicate and one field of view/well was captured and analyzed as described below.

Zebrafish ISV and CVP image analysis

Segmentation and feature extraction algorithms were developed to analyze images of exposed zebrafish embryos for the two most common malformations, ISV morphology (ISV count; average distance between ISV; total area of ISV; and average ISV length) and condensation of CVP (shape quantification of CVP and fenestrations) (Supplementary Figure 1), as have been described previously [37, 38]. Briefly, the algorithms extracts whole zebrafish embryos from images, while excluding other objects, such as the edges of well plates using triangle thresholding [39]. The position of the zebrafish embryo in the image is normalized by placing the longest axis of a fitted ellipse parallel to the horizontal axis. The zebrafish image is bisected into ISV + DLAV region and tail + head region using intermodes thresholding based on bimodal distribution [40]. The isolated portions of the head and yolk regions are masked out using the skeleton of the segmented region containing ISV + DLAV. A segmentation method incorporating vessel direction and the eigenvector of the Hessian matrix is used for vessel detection and to obtain a segmented vessel tree. ISV count; average distance between ISV; total area of ISV; and average ISV length are calculated from segmented ISV. The automatic segmentation was compared to manual segmentation by two different users, each provided with 30 randomly chosen ISV images. Users visually inspected the ISV images and marked the pixels belonging to ISV with paint using the NET software (http://www.getpaint.net/index.html). The output of the segmentation comparison is a binary vector with the same size as the image. A true positive is when output of automated segmentation is 1 when manual users marked it as 1; a true negative is when the output of the automated segmentation is 0 when the manual users labeled it as 0; a false positive is when the output of the automated segmentation is 1 while users labeled it as 0; and a false

negative is when the output of the automated segmentation is 0 while the users labeled it as 1. Accuracy is defined as ratio of sum of true positives and true negatives over sum of true positives, true negatives, false positives and false negatives. The average accuracy for the ISVs with manual users was 0:952 and 0:951, respectively. Average f-score, which represents area overlap between manual and automated segmentation, for the users were 0.830 and 0.832.

For the analysis of the perturbed CVP condensation, the segmentation extracts the CV region from an individual zebrafish embryo by smoothing the image with Gaussian filter. Similar to ISV, after bisection of zebrafish into two regions, ISV + DLAV region and tail + head region, the skeleton of the segmented image is used to remove head from tail + head region. The CVP region is isolated using curvature analysis. Shape of CVP is quantified using gradient weighted co-occurrence of histogram of oriented gradients (gCo-HOG). The measurements include numbers, average distances, average areas and total area of fenestrations, as well as numbers of fenestrations, total area, orientation diameter, perimeter and solidity of CVP.

To identify perturbed vasculature, machine learning was applied, as previously described [41]. Briefly, for identification of ISV perturbations, the quantified features described above were used to train a linear support vector machine (SVM) classifier to identify morphological changes in a dataset consisting of consisting of 380 images (190 with normal ISVs and 190 with perturbed ISVs). One-third of the data was used for parameter estimation for SVM and the remaining two-thirds for training and testing. Parameters were determined based on a grid-search that was conducted with 3-fold cross-validation, using the parameter values that achieved the best cross-validation accuracy. Cross-validation is an approach to evaluate performance of a classifier by partitioning the original sample into a training set to train the model, and a test set to evaluate it. In 3-fold cross-validation, the data set is randomly partitioned into 3 equally sized sub samples, following which a set of 3 experiments is performed as follows: two subsamples are used for training and one is used for testing. Each of the 3 subsamples is used exactly once for testing. To identify perturbed CVP, we utilized gCo-HOG features to train a linear SVM classifier. The dataset for the CVP consisted of 180 images (90 with normal and 90 with abnormal CVP). Similarly to the ISV analysis, the data was split into parts for parameter estimation and training and testing. Using the parameter values that achieved the best cross-validation accuracy, 2039 zebrafish images were analyzed for ISV and CVP perturbations.

In up to 10% of the segmented images (with one fish/image), our algorithm failed to correctly identify ISV/CVP regions due to image noise or algorithm limitations. Hence, we applied a cut-off at 10% of the embryo population and did not consider effects below 10% to be a perturbation.

Mouse C166 tube formation assay image analysis

For analysis, images were converted to RGB format. Angiogenesis analyzer for Image J was used to determine the capability of C166 cells to assemble into capillary-like structures [42]. The macro is available at http://imagej.nih.gov/ij/macros/toolsets/Angiogenesis%20Analyzer.txt and more information can be found at http://image.bio.methods.free.fr/

ImageJ/?Angiogenesis-Analyzer-for-ImageJ. A test chemical was determined to disrupt the capability of C166 to form capillary-like structures on Matrigel if it affected any of the 20 parameters quantified by angiogenesis analyzer. Based on triplicate samples, statistically significant ($P<0.05$) effects were determined by Students t-test.

Putative VDC signatures for the identified VDCs

A putative VDC (pVDC) signature for each chemical was visualized using EPA's Toxicological Prioritization Index (ToxPi) tool [43] and used to rank the tested chemicals based on each chemical's predicted ability to disrupt blood vessel formation. The pVDC ToxPi signatures for ToxCast phase I chemicals were generated previously based on data mining of genetic mouse models where disruption of vascular development was associated with adverse prenatal outcomes combined with HTS data tested on mechanistic *in vitro* assays related to these genes [5, 33]. The pVDC signature used in this study is based on the published AOP for embryonic vascular disruption [5], but has been modified to include additional assay data on critical vascular developmental targets. It consists of 124 HTS assays linked to 30 molecular targets assays that span a wide range of biology relevant to angiogenesis, including VEGFR-dependent signaling, vessel remodeling, extra cellular matrix interactions, chemokine signaling pathways, and estrogen receptor pathway activation, as well as assays that measure proliferation and viability of human primary vascular cells (endothelial and smooth muscle) (Tal et al., RTX submitted manuscript to this issue 2016). The ToxPi graphic represents component slices of a unit circle, with each slice containing information on a particular vascular developmental target (between 1–17 assays per slice). The assay target potency is represented by the slice distance from the origin, and all slices were set to have equal weight. The ToxPi program also sums a pVDC score for each chemical from the component slices of a unit circle, as described in [43]. The output was normalized such that pVDC scores were between 0 and 1, where a score of 1 would indicate a chemical with the highest possible potency against every assay/target in every slice (the top pVDC from ToxCast Phase I had a ToxPi score of 0.498). Average ToxPi scores for all chemicals tested were calculated.

Results

Identification of compounds from ToxCast Phase I chemical library that disrupt embryonic vascular development in zebrafish

To identify whether chemicals from ToxCast Phase I library impair blood vessel development *in vivo*, we tested 161 chemicals from this library in the zebrafish assay. We found that chemical exposures caused a plethora of perturbations in the formation of major vasculature networks, such as ISV, DA, and CVP, as well as induced other cardiotoxicity phenotypes, such as pericardial edema, hemorrhages and thrombosis (Figure 1). Under normal conditions, ISVs from either side of the embryo extend dorsally from the DA to the DLAV and overlap one another when imaged laterally (Figure 1A). Chemically induced abnormalities included the presence of non-overlapping ISVs from the left and right side of the embryo (Figure 1B), or thin and underdeveloped ISV (Figure 1C). DA/PCV aberration represented an expansion of the vessel (Figure 1D). By 72 hpf, the CVP is condensed to a thinner vessel network (Figure 1E). Exposure-induced CVP defects typically included an

expanded and less condensed CVP with several wide fenestrations (Figure 1F), or a misshapen CVP network (Figure 1G). Several compounds caused pericardial edema (Figure 1H), which typically is associated with an obstructed venous or lymphatic system, increased vascular permeability or cardiac failure, resulting in an excessive/abnormal volume of fluid in the space surrounding heart chambers. Compounds also caused hemorrhages, or pools of blood in a tissue, which can be caused by the rupture of blood vessels, and thrombosis, which was represented by the formation of a blood clot [44]. Of the 161 screened compounds, 34 chemicals induced discernible vascular disruption, as visually determined (Table 1 and Supplementary Table S2).

For the 34 chemicals visually identified as VDCs, automated quantitative image analysis was performed on microscope images of the embryos for the two most commonly affected vascular disruption endpoints: perturbation of ISVs and CVP (Supplementary Figure 1) [37, 38]. The percentage of embryos in a treatment group with perturbed vasculature for either ISVs or CVP was recorded. The Lowest Effect Level (LEL) for each chemical is shown in Table 1. The percentage of affected embryos for all chemicals across all doses tested is shown in Supplementary Figure S2.

The chemicals were grouped into two categories based on quantitative image analysis, as those which affected both ISV and CVP, and those that affected CVP only (Table 1). Twenty-two of the 34 VDCs perturbed both ISV and CVP formation and 6 VDCs affected the condensation of the CVP only. Rotenone, oryzalin, trifloxystrobin and pyraclostrobin had the lowest LELs for ISV perturbations according to the image analysis-based quantification, while endosulfan, rotenone and tribufos had the lowest LELs for CVP disruption. Six of the compounds did not have any quantifiable effect above 10% on either ISV or CVP formation, despite being visually classified as VDCs. These compounds included dibutyl phthalate, quinoxyfen, flumetralin and chlorpyrifos oxon, which perturbed CVP formation according to the visual determination, and butafenacil and lactofen, which both caused pericardial edema, an endpoint not covered by the image analysis. Of the four compounds that were visually scored to have uncondensed CVP, three showed a small CVP effect by image analysis, but fell below our 10% cutoff value, and therefore they were categorized as non-VDCs.

Perturbations of tube formation in mouse C166 endothelial cells

As expected, C166 cells formed capillary-like structures when placed on the Matrigel basement membrane matrix (Figure 2). This tube formation assay using C166 cells was used to screen the 34 VDCs initially identified in zebrafish by visual determination. The effect of these chemicals on the capability of C166 cells to form capillary-like structures was determined with angiogenesis analyzer. An example of the output generated by angiogenesis analyzer upon quantification of a tube formation assay experiment images of C166 cells exposed to rotenone is shown in Figure 2.

Each of the 34 VDCs identified in zebrafish was tested in the tube formation assay with C166 cells. An example of data generated from the tube formation assay for all quantified parameters for rotenone is provided in Supplementary Figure S3. The minimal concentration required to affect any parameter was recorded as the LEL. Overall, 28 compounds out of the

34 VDCs visually identified in the zebrafish assay were determined as VDCs in C166 cells (Figure 3). Of the compounds 22 compounds that were identified as VDCs based on image analysis, 20 compounds affected C166 angiogenesis. The VDCs with the lowest LEL according to this assay were cyazofamid, pyraclostrobin, tebufenpyrad and fenpyroximate. Six compounds were inactive in the C166 cell assay (allethrin, cymoxanil, dimethomorph, esfenvalerate, malaoxon, and oryzalin).

Putative Vascular Disruptor Compound signatures for the identified VDCs

We compared the HTS bioactivity profiles of the chemicals identified as VDCs in both zebrafish and C166 cells using the ToxPi tool [42]. We used a pVDC signature that incorporated 124 high throughput assays linked to 30 molecular targets (Figure 4A) to generate pVDC signatures for the 161 chemicals, and rank the compounds by their computed ToxPi scores (Figure 4B and C), which predicted how likely it is that a compound would have a vascular disruptive effect. The analysis visualized that the compounds that perturbed ISV development in zebrafish and tube formation in C166 cells also interfered with chemokine signaling, extracellular matrix components, and the vascular endothelial growth factors, particularly VEGFR2, in the ToxCast *in vitro* assays (Figure 4B). The average ToxPi score for the 22 chemicals that perturbed vascular development both in zebrafish (by machine learned image analysis) and tube formation in C166 cells was 0.202. The most potent pVDC according to the ranking was niclosamide with a ToxPi score of 0.411. The group of chemicals that perturbed blood vessel formation in only one of the model systems, either in zebrafish or in C166 cells, had an average ToxPi score of 0.16. The average ToxPi score for chemicals classified as non-VDCs by zebrafish screening was 0.109.

Discussion

Since the discovery that anti-angiogenic compounds repress tumor vascularization and growth, there has been an ongoing search for anti-angiogenic compounds to use in cancer therapies (reviewed in [45]). Simultaneously, awareness has arisen of the potential teratogenic effects of certain pharmaceuticals and other vascular disruptive agents [5]. The EPA's ToxCast program has provided an initial prioritization of environmental compounds based on their activity as potential VDCs [33]. However, a systematic experimental search for VDCs among environmental pollutants using functional *in vivo* and multicellular models had not been undertaken.

We here have performed the largest *in vivo* screen to date for VDCs among known environmental chemicals. While the initial visual zebrafish screen identified 34 VDCs, the quantitative image analysis-based zebrafish screen identified 28 VDCs. The secondary screen in C166 cells found that 20 of these compounds perturbed *in vitro* tubule formation. In addition, two of the compounds that caused pericardial edema in zebrafish, an endpoint not quantified by the zebrafish image analysis program, were VDCs in C166 cells. Thus in total, 22 compounds were identified to have vascular disrupting activity both in zebrafish and C166 cells. The discrepancy between the results in zebrafish and in mouse cells may be caused by alternative molecular mechanisms by which certain compounds affect angiogenesis between the two systems. It is also possible that species-specific effects of the

compounds contribute to the differences. Another plausible explanation for the differences in effects is that we compared an *in vivo* model to an *in vitro* model; considering that in vitro assays may have limited metabolic capacity, compounds requiring biotransformation may be active only in the zebrafish model. In addition, the uptake of certain compounds in fish could be different than in the immortalized C166 cells. Furthermore, other developmental perturbations in fish besides vascular disruption, such as a stunted tail growth, may produce the CVP phenotype. Extended time-lapse microscopy of vascular development in zebrafish demonstrates that the CVP condenses as the fish tail extends [46]. Thus, the CVP phenotype may not only be a direct causality from vascular disruption, but it may also represent false positives in the zebrafish VDC screen.

Zebrafish angiogenesis is regulated by an array of molecular signals, such as vascular endothelial growth factor (VEGF-A) and its receptors, VEGFR2 and neuropilin-1 (Nrp1) [47, 48]. Stimulation of VEGF-A signaling has been shown to promote the growth and migration of endothelial cells in ISV development [49]. Further interaction with notch signaling is also required for perfecting proper ISV patterning [50]. On the other hand, angiogenesis in the zebrafish CVP takes on a slightly different set of molecular signals that includes phosphoinositide 3-kinase (Pi3k), VEGF-C/Flt4 and ephrin receptor B4 (Ephb4) [51]. To obtain initial information on which molecular initiating events were affected by the identified VDCs, we compared the pVDC ToxPi signatures of the compounds with vascular disruption activity to those without. The comparison showed that HTS assays that test for chemical disruptors of cytokines, especially chemokine (C-C motif) ligand 2 (CCL2), extracellular matrix composition, and VEGF signaling, in particular via VEGFR2, were often altered by the compounds that produced vascular toxicity. For VEGFR2, 50% of the chemicals that were VDCs in zebrafish and C166 cells disrupted VEGFR2 signaling in the ToxCast assays. This can be compared to a hit rate of 15.7% against the VEGFR2 target for the entire ToxCast library overall [52]. Our previous targeted study with PTK787, a VEGFR2 kinase inhibitor, elucidated an AOP for vascular disruption and developmental toxicity in the zebrafish platform [27]. On the other hand, other HTS assays present in the VDC ToxPi signature were seldom hit. One such example is the assay for the angiopoietin receptor Tie2. While Tie2 is crucial for angiogenesis in the mouse fetus (reviewed in [53]), in zebrafish its main role is rather in maintaining vessel integrity after its formation [54], which may explain why it did not emerge as a target in our analysis. The average ToxPi score for the zebrafish and C166 VDCs (0.202) was higher than for the compounds not identified as VDCs in zebrafish (0.109), confirming that the predictive pVDC signature can be used to rank VDCs. However, this pVDC signature is inherently limited by molecular targets that have corresponding *in vitro* assays in the ToxCast program, and thus do not reflect all possible pathways involved in vascular development.

One such example of relevant biology potentially missing from the pVDC signature is mitochondrial function. The most highly ranked compound by ToxPi was niclosamide; exposure to niclosamide, a salicyanilide compound, disrupts the mitochondrial membrane potential and reduces ATP levels in cells [55]. Additional VDCs identified here *in vivo* and *in vitro*, including abamectin, pyridaben, fenpyroxymate, endosulfane, pyraclostrobin, tebufenpyrad, rotenone, trifloxystrobin , tribufos, and 2,4-dichlorophenoxyacetic acid, are all known to disrupt mitochondrial function in various cells and species [56–63]. Of these,

pyridaben, fenpyroxymate, tebufenpyrad, and rotenone inhibit Complex I of the electron transport chain, while pyraclostrobin and trifloxystrobin inhibit respiratory Complex III. Corroborating the importance of Complex III for angiogenesis, knock down or chemical inhibition of ubiquinol-cytochrome c reductase binding protein (Uqcrb), a Complex III subunit, in zebrafish inhibits ISV angiogenesis and suppresses VEGF levels [64]. It should be noted that inhibition of mitochondrial function is a relatively common mechanism of action for pesticides, and the correlation between mitochondrial disruptive activity and high VDC ranking might be ancillary. Future studies are needed to investigate the interplay between vascular and mitochondrial disruption.

Many of the ToxCast Phase I chemicals have previously been analyzed for developmental toxicity in rodents (animal toxicity data downloadable from https://www.epa.gov/chemical-research/toxicity-forecaster-toxcasttm-data). Fifty-five percent of the VDCs that perturbed both zebrafish and C166 vascular development also caused fetal malformations in rat. Whether any of these malformations can be linked to vascular disruption is currently not known, because vascular disruption per se was not assessed in the rat studies. Thus, research will be needed to find out whether the VDCs identified here also affect vascular development in mammals. More research is also required to be able to compare effect doses between rodents and zebrafish. Difficulties for comparing doses between species include differences in exposure routes and compound uptake, as well as potential species-specific biotransformation.

Our screening of a subset of the ToxCast Phase I chemicals identified 22 novel vascular disruptors, some of which were active at nanomolar concentrations. It also showed that among 161 environmental compounds, we found a high proportion (14%) of compounds with vascular disruption capacity compared to other screens performed on drug and small chemical libraries [65, 66]. Out of the top ranked compounds for pVDC capacity in Kleinstreuer et al. [33] we identified 30% as VDCs in zebrafish and C166 cells. We conclude that complementary HTS models, such as those of the present study, can be used to further prioritize chemicals for testing in mammals from the chemicals ranked by pVDC scores from the ToxCast screening program.

Supplementary Material

Refer to Web version on PubMed Central for supplementary material.

Acknowledgments

We thank Sharanya Maanasi Kalasekar for help with making figures. This work was supported by grants from the Environmental Protection Agency (grant numbers R834289 and R83516301), the National Institute of Environmental Health Sciences of the National Institutes of Health (grant number P30ES023512 and contract number HHSN273201500010C), the Robert A Welch Foundation (grant number E-0004) and the Emerging Technology Fund of Texas under Agreement 300-9-1958. The content is solely the responsibility of the authors and does not necessarily reflect the views of the funding agencies.

Abbreviations

HTS	High throughput screening

ECs	Endothelial cells
DA	Dorsal aorta
PCV	Posterior cardinal vein
hpf	Hours post fertilization
ISVs	Intersegmental vessels
DLAV	Dorsal longitudinal anastomotic vessel
CV	Caudal vein
CVP	Caudal vein plexus
pVDCs	Putative vascular disruptor compounds
AOP	Adverse outcome pathway
SVM	Support vector machine
ToxPi	Toxicological Prioritization Index
LEL	Lowest Effect Level
VEGF	Vascular endothelial growth factor

References

1. Bergman A, et al. The impact of endocrine disruption: a consensus statement on the state of the science. Environ Health Perspect. 2013; 121(4):A104–A106. [PubMed: 23548368]
2. Diamanti-Kandarakis E, et al. Endocrine-disrupting chemicals: an Endocrine Society scientific statement. Endocr Rev. 2009; 30(4):293–342. [PubMed: 19502515]
3. Kabir ER, Rahman MS, Rahman I. A review on endocrine disruptors and their possible impacts on human health. Environ Toxicol Pharmacol. 2015; 40(1):241–258. [PubMed: 26164742]
4. Miller MD MM, Landrigan PJ. Children's Environmental Health: Beyond National Boundaries. Pediatr Clin North Am. 2016; 63(1):149–165. [PubMed: 26613694]
5. Knudsen TB, Kleinstreuer NC. Disruption of embryonic vascular development in predictive toxicology. Birth Defects Res C Embryo Today. 2011; 93(4):312–323. [PubMed: 22271680]
6. Van Allen MI. Structural anomalies resulting from vascular disruption. Pediatr Clin North Am. 1992; 39(2):255–277. [PubMed: 1553243]
7. Therapontos C, et al. Thalidomide induces limb defects by preventing angiogenic outgrowth during early limb formation. Proc Natl Acad Sci U S A. 2009; 106(21):8573–8578. [PubMed: 19433787]
8. Ahmed S, et al. Arsenic-associated oxidative stress, inflammation, and immune disruption in human placenta and cord blood. Environmental health perspectives. 2011; 119(2):258–264. [PubMed: 20940111]
9. Fei DL, et al. Association between in utero arsenic exposure, placental gene expression, and infant birth weight: a US birth cohort study. Environmental health : a global access science source. 2013; 12:58. [PubMed: 23866971]
10. Remy S, et al. Expression of the sFLT1 gene in cord blood cells is associated to maternal arsenic exposure and decreased birth weight. PloS one. 2014; 9(3):e92677. [PubMed: 24664213]
11. Coultas L, Chawengsaksophak K, Rossant J. Endothelial cells and VEGF in vascular development. Nature. 2005; 438(7070):937–945. [PubMed: 16355211]

12. Cowden Dahl KD, et al. Hypoxia-inducible factors 1alpha and 2alpha regulate trophoblast differentiation. Mol Cell Biol. 2005; 25(23):10479–10491. [PubMed: 16287860]
13. Hiratsuka S, et al. Membrane fixation of vascular endothelial growth factor receptor 1 ligand-binding domain is important for vasculogenesis and angiogenesis in mice. Mol Cell Biol. 2005; 25(1):346–354. [PubMed: 15601855]
14. Imanishi S, et al. Prenatal exposure to permethrin influences vascular development of fetal brain and adult behavior in mice offspring. Environmental toxicology. 2013; 28(11):617–629. [PubMed: 24150868]
15. Tait S, et al. Bisphenol A affects placental layers morphology and angiogenesis during early pregnancy phase in mice. J Appl Toxicol. 2015
16. Bonventre JA, White LA, Cooper KR. Methyl tert butyl ether targets developing vasculature in zebrafish (Danio rerio) embryos. Aquat Toxicol. 2011; 105(1–2):29–40. [PubMed: 21684239]
17. McCollum CW, et al. Embryonic exposure to sodium arsenite perturbs vascular development in zebrafish. Aquat Toxicol. 2014; 152:152–163. [PubMed: 24768856]
18. McCollum CW, et al. Developmental toxicity screening in zebrafish. Birth Defects Res C Embryo Today. 2011; 93(2):67–114. [PubMed: 21671351]
19. Ackermann GE, Paw BH. Zebrafish: a genetic model for vertebrate organogenesis and human disorders. Frontiers in bioscience : a journal and virtual library. 2003; 8:d1227–d1253. [PubMed: 12957827]
20. Filby AL, Ortiz-Zarragoitia M, Tyler CR. The vas::egfp transgenic zebrafish: a practical model for studies on the molecular mechanisms by which environmental estrogens affect gonadal sex differentiation. Environmental toxicology and chemistry / SETAC. 2014; 33(3):602–605.
21. Galloway JL, Zon LI. Ontogeny of hematopoiesis: examining the emergence of hematopoietic cells in the vertebrate embryo. Curr Top Dev Biol. 2003; 53:139–158. [PubMed: 12510667]
22. Zhong TP, et al. Gridlock signalling pathway fashions the first embryonic artery. Nature. 2001; 414(6860):216–220. [PubMed: 11700560]
23. Isogai S, Horiguchi M, Weinstein BM. The vascular anatomy of the developing zebrafish: an atlas of embryonic and early larval development. Developmental biology. 2001; 230(2):278–301. [PubMed: 11161578]
24. Choi J, et al. Aplexone targets the HMG-CoA reductase pathway and differentially regulates arteriovenous angiogenesis. Development. 2011; 138(6):1173–1181. [PubMed: 21307094]
25. Mouillesseaux K, Chen JN. Mutation in utp15 disrupts vascular patterning in a p53-dependent manner in zebrafish embryos. PloS one. 2011; 6(9):e25013. [PubMed: 21949834]
26. Cha YR, Weinstein BM. Visualization and experimental analysis of blood vessel formation using transgenic zebrafish. Birth Defects Res C Embryo Today. 2007; 81(4):286–296. [PubMed: 18228261]
27. Tal TL, et al. Immediate and long-term consequences of vascular toxicity during zebrafish development. Reprod Toxicol. 2014
28. Arnaoutova I, Kleinman HK. In vitro angiogenesis: endothelial cell tube formation on gelled basement membrane extract. Nature protocols. 2010; 5(4):628–635. [PubMed: 20224563]
29. Ades EW, et al. HMEC-1: establishment of an immortalized human microvascular endothelial cell line. The Journal of investigative dermatology. 1992; 99(6):683–690. [PubMed: 1361507]
30. O'Connell KA, Edidin M. A mouse lymphoid endothelial cell line immortalized by simian virus 40 binds lymphocytes and retains functional characteristics of normal endothelial cells. Journal of immunology. 1990; 144(2):521–525.
31. Wang SJ, Greer P, Auerbach R. Isolation and propagation of yolk-sac-derived endothelial cells from a hypervascular transgenic mouse expressing a gain-of-function fps/fes proto-oncogene. In vitro cellular & developmental biology. Animal. 1996; 32(5):292–299. [PubMed: 8792159]
32. Hughes CS, Postovit LM, Lajoie GA. Matrigel: a complex protein mixture required for optimal growth of cell culture. Proteomics. 2010; 10(9):1886–1890. [PubMed: 20162561]
33. Kleinstreuer NC, et al. Environmental impact on vascular development predicted by high-throughput screening. Environ Health Perspect. 2011; 119(11):1596–1603. [PubMed: 21788198]

34. Kleinstreuer N, et al. A computational model predicting disruption of blood vessel development. PLoS Comput Biol. 2013; 9(4):e1002996. [PubMed: 23592958]
35. Westerfield, M. A zebrafish book. A guide for the laboratory use of zebrafish (Danio rerio). 5th. Eugene: University of Oregon Press; 2007.
36. Kimmel CB, et al. Stages of embryonic development of the zebrafish. Developmental dynamics : an official publication of the American Association of Anatomists. 1995; 203(3):253–310. [PubMed: 8589427]
37. Hans C, et al. Automated analysis of zebrafish images for screening toxicants. Conf Proc IEEE Eng Med Biol Soc, 2013. 2013:3004–3007.
38. Hans C, et al. Gradient Weighted Co-Hog for Analysis of Caudal Vein Structural Changes in Toxin Exposed Zebrafish Embryo. The International Symposium on Biomedical Imaging (ISBI). 2015
39. Zack GW, Rogers WE, Latt SA. Automatic measurement of sister chromatid exchange frequency. J Histochem Cytochem. 1977; 25(7):741–753. [PubMed: 70454]
40. Prewitt JM, Mendelsohn ML. The analysis of cell images. Ann N Y Acad Sci. 1966; 128(3):1035–1053. [PubMed: 5220765]
41. Hans C. Image analysis for zebrafish vasculature. Thesis, University of Houston. 2015
42. Schneider C, Rasband W, Eliceiri K. NIH Image to ImageJ: 25 years of image analysis. Nature Methods. 2012; 9:671–675. [PubMed: 22930834]
43. Reif DM, et al. Endocrine profiling and prioritization of environmental chemicals using ToxCast data. Environ Health Perspect. 2010; 118(12):1714–1720. [PubMed: 20826373]
44. McGrath, P. Zebrafish. John Wiley & Sons, Inc; 2011. Use of Emerging Models for Developmental Toxicity Testing; p. 27-44.
45. Phung MW, Dass CR. In-vitro and in-vivo assays for angiogenesis-modulating drug discovery and development. J Pharm Pharmacol. 2006; 58(2):153–160. [PubMed: 16451742]
46. Kaufmann A, et al. Multilayer mounting enables long-term imaging of zebrafish development in a light sheet microscope. Development. 2012; 139(17):3242–3247. [PubMed: 22872089]
47. Habeck H, et al. Analysis of a zebrafish VEGF receptor mutant reveals specific disruption of angiogenesis. Current biology : CB. 2002; 12(16):1405–1412. [PubMed: 12194822]
48. Lee P, et al. Neuropilin-1 is required for vascular development and is a mediator of VEGF-dependent angiogenesis in zebrafish. Proceedings of the National Academy of Sciences of the United States of America. 2002; 99(16):10470–10475. [PubMed: 12142468]
49. Holden BJ, Bratt DG, Chico TJ. Molecular control of vascular development in the zebrafish. Birth defects research. Part C, Embryo today : reviews. 2011; 93(2):134–140.
50. Hellstrom M, et al. Dll4 signalling through Notch1 regulates formation of tip cells during angiogenesis. Nature. 2007; 445(7129):776–780. [PubMed: 17259973]
51. Herbert SP, et al. Arterial-venous segregation by selective cell sprouting: an alternative mode of blood vessel formation. Science. 2009; 326(5950):294–298. [PubMed: 19815777]
52. Kleinstreuer NC, et al. Phenotypic screening of the ToxCast chemical library to classify toxic and therapeutic mechanisms. Nat Biotechnol. 2014; 32(6):583–591. [PubMed: 24837663]
53. Ward NL, Dumont DJ. The angiopoietins and Tie2/Tek: adding to the complexity of cardiovascular development. Semin Cell Dev Biol. 2002; 13(1):19–27. [PubMed: 11969368]
54. Gjini E, et al. Zebrafish Tie-2 shares a redundant role with Tie-1 in heart development and regulates vessel integrity. Disease Model Mechanisms. 2011; 4(1):57–66.
55. Park SJ, et al. Niclosamide induces mitochondria fragmentation and promotes both apoptotic and autophagic cell death. BMB Rep. 2011; 44(8):517–522. [PubMed: 21871175]
56. Dubey RK, Beg MU, Singh J. Effects of endosulfan and its metabolites on rat liver mitochondrial respiration and enzyme activities in vitro. Biochem Pharmacol. 1984; 33(21):3405–3410. [PubMed: 6149750]
57. Maioli MA, et al. The role of mitochondria and biotransformation in abamectin-induced cytotoxicity in isolated rat hepatocytes. Toxicol In Vitro. 2013; 27(2):570–579. [PubMed: 23142325]
58. Melnick RL, Schiller CM. Effect of phthalate esters on energy coupling and succinate oxidation in rat liver mitochondria. Toxicology. 1985; 34(1):13–27. [PubMed: 3969678]

59. Mirakhmedov AK, et al. Effect of defoliant (butiphose) on morpho-physiological properties and enzyme systems of natural membranes. Indian J Exp Biol. 1989; 27(3):245–247. [PubMed: 2606532]

60. Navarro A, et al. Effects of rotenone and pyridaben on complex I electron transfer and on mitochondrial nitric oxide synthase functional activity. J Bioenerg Biomembr. 2010; 42(5):405–412. [PubMed: 20886364]

61. Oakes DJ, Pollack JK. Effects of a herbicide formulation, Tordon 75D, and its individual components on the oxidative functions of mitochondria. Toxicology. 1999; 136(1):41–52. [PubMed: 10499849]

62. Schuler F, Casida JE. The insecticide target in the PSST subunit of complex I. Pest Manag Sci. 2001; 57(10):932–940. [PubMed: 11695186]

63. Shiraishi Y, et al. Fenpyroximate binds to the interface between PSST and 49 kDa subunits in mitochondrial NADH-ubiquinone oxidoreductase. Biochemistry. 2012; 51(9):1953–1963. [PubMed: 22353032]

64. Cho YS, et al. Functional inhibition of UQCRB suppresses angiogenesis in zebrafish. Biochem Biophys Res Commun. 2013; 433(4):396–400. [PubMed: 23454382]

65. Kitambi SS, et al. Small molecule screen for compounds that affect vascular development in the zebrafish retina. Mech Dev. 2009; 126(5–6):464–477. [PubMed: 19445054]

66. Tran TC, et al. Automated, quantitative screening assay for antiangiogenic compounds using transgenic zebrafish. Cancer Res. 2007; 67(23):11386–11392. [PubMed: 18056466]

Highlights

- Vascular disruptors were identified through screening in zebrafish embryos and mouse C166 cells
- In zebrafish, exposure to the compounds caused a plethora of malformations of the vasculature
- In C166 mouse embryonic endothelial cells, exposure to the compounds inhibited tube formation
- By computational toxicity, putative molecular targets for the compounds were predicted

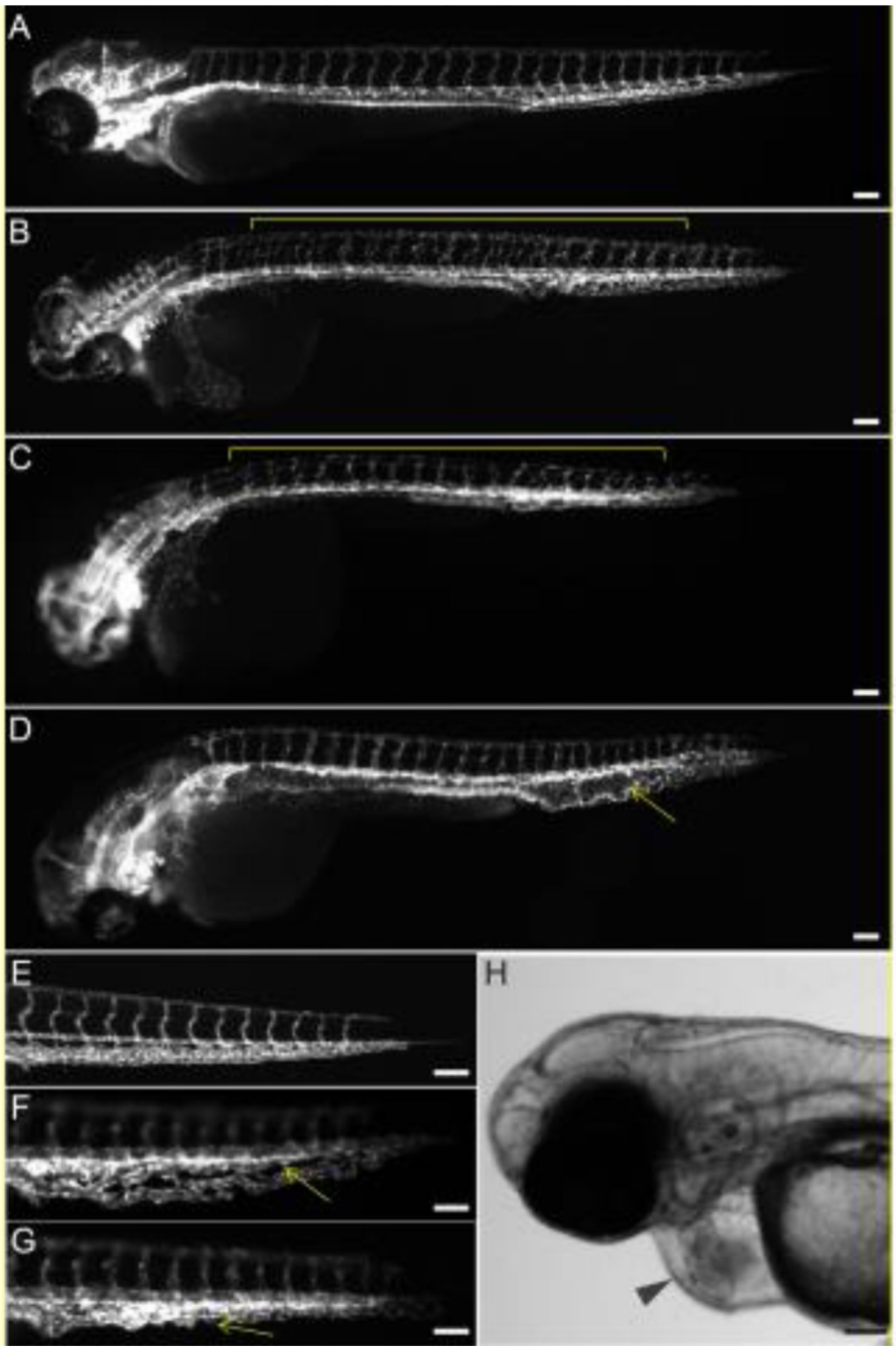

Figure 1.

VDCs cause malformed vascular development in the ISV, DA and CVP.

Tg(kdrl:EGFP)mitfa^{b692} embryos were treated with vehicle (control; A, E) or chemicals from the ToxCast Phase 1 chemical library (B-D, F, G) from 3 hpf to 72 hpf. Lateral view with anterior to the left and dorsal to the top. Vascular defects include non-overlapping ISVs (B), or thin and underdeveloped ISVs (C), expanded DA (D), and less condensed CVP (F), or misshapen CVP (G) and are marked with yellow lines or arrows. A common vascular-

related phenotype, which is characteristic of cardiotoxicity, is pericardial edema (H; black arrowhead). Scale bar = 100 μm.

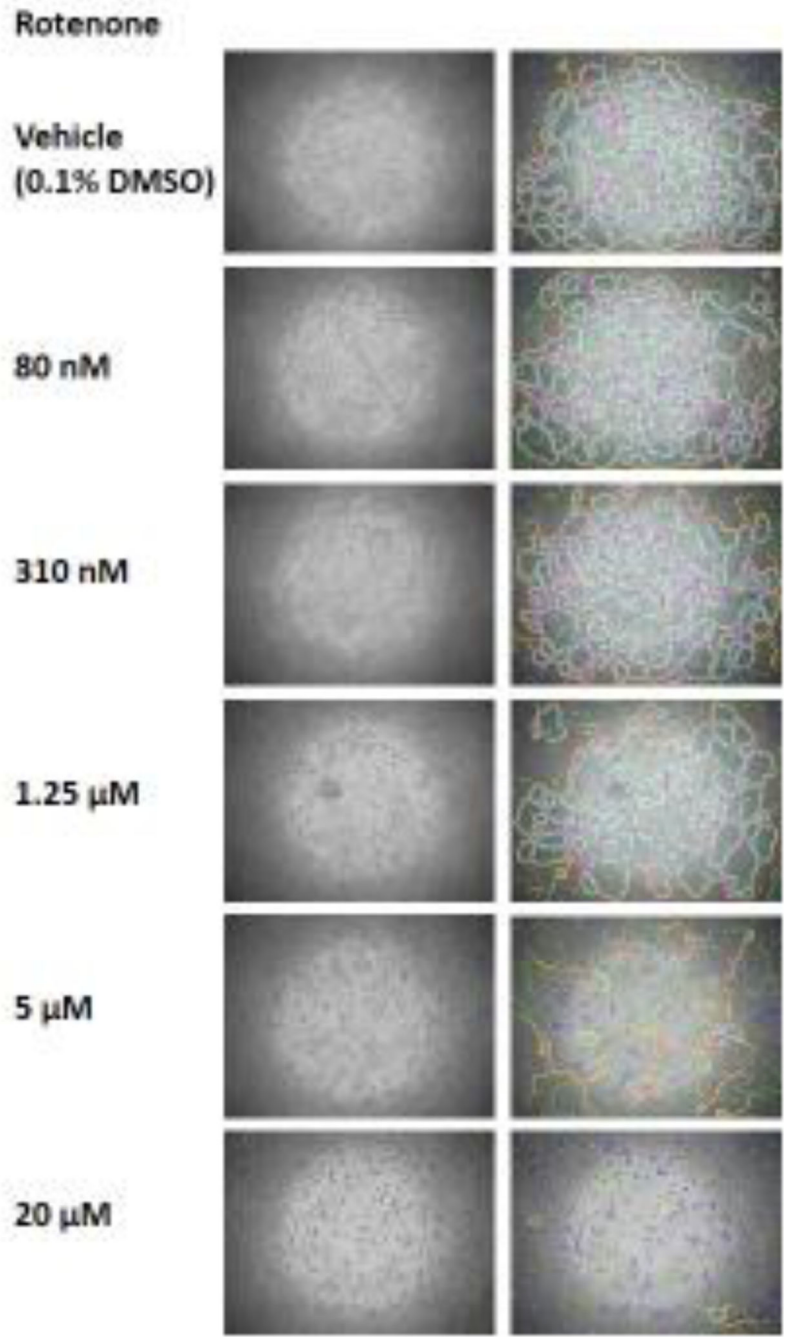

Figure 2.

C166 cells tube formation is affected by VDCs. C166 cells assemble into capillary-like structures when grown on Matrigel for 150 minutes. Angiogenesis analyzer mapping of the mesh network formed by C166 cells growing on Matrigel upon treatment with vehicle (0.1% DMSO) and increasing doses of rotenone for 150 minutes.

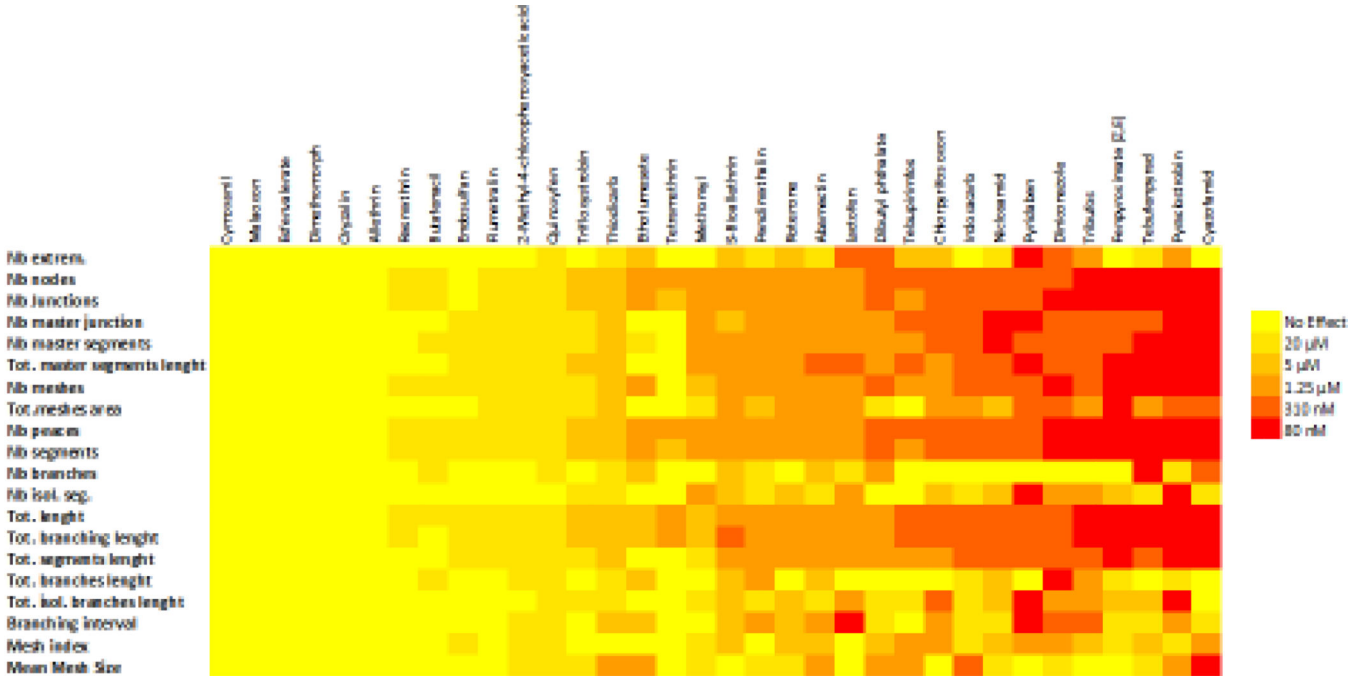

Figure 3.

The color map shows the minimal concentration of each chemical required to affect in a dose-dependent manner the parameters measured by angiogenesis analyzer in C166 cells.

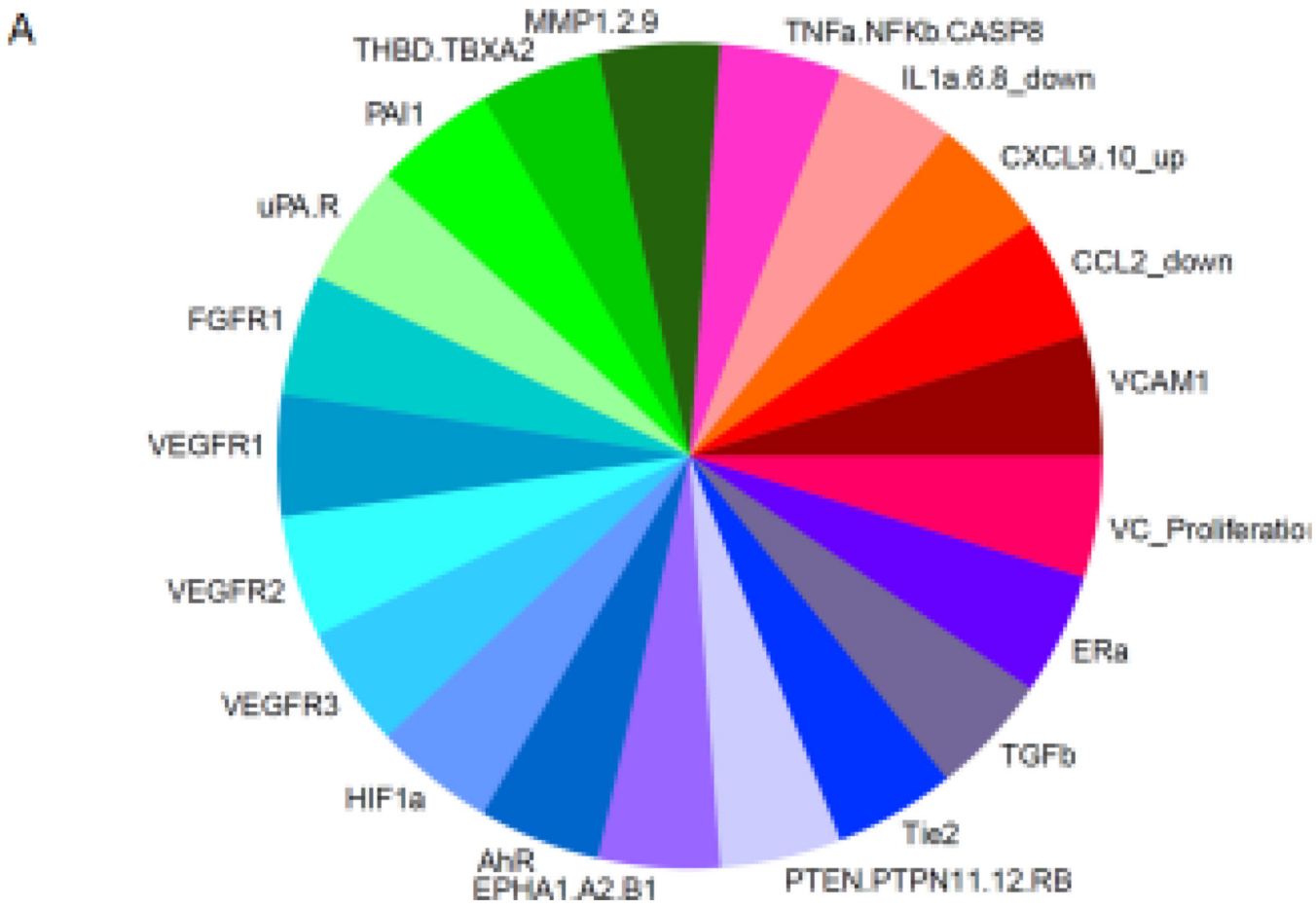

Figure 4.

pVDC signatures for zebrafish and C166 cell VDCs. Molecular pathways with corresponding *in vitro* assays used in the ToxCast screening program that were selected to build the putative VDC signature (A). Ranking and pVDC signatures of VDCs active both in zebrafish and in C166 cells (B). Ranking and pVDC signatures of chemicals acting as VDCs in either zebrafish or C166 cells (C). Cytokine signaling (red); vessel stabilization (purple),

angiogenic signaling (blue); and extracellular matrix (ECM) remodeling (green) quadrants are shown.

Reprod Toxicol. Author manuscript; available in PMC 2018 June 01.

Table 1

Lowest effect levels (LELs) for compounds that cause ISV and PVC perturbations in zebrafish by quantitative image analysis

Chemical name	LEL for ISV perturbations (μM)	Embryos with perturbed ISVs at LEL (%)	LEL for CVP perturbations (μM)	Embryos with perturbed CVP at LEL (%)	Effect by visual determination
2-methyl-4-chloro phenoxyacetic acid	No effect *		10	18	PE
Abamectin	1	100	1	10	PE
Allethrin	10	67	1	20	PE, BC
Butafenacil	No effect		No effect		PE
Chlorpyrifos oxon	No effect		No effect		CVP
Cyazofamid	0.5	44	0.5	56	CVP
Cymoxanil	20	12	10	86	CVP, PE, BC
Dibutyl phthalate	No effect		No effect		CVP
Dimethomorph	No effect		20	11	CVP
Diniconazole	5	14	5	14	DA/PCV, PE
Endosulfan	1	42	0.01	28	CVP
Esbiol (S-Bioallethrin)	5	12	1	10	CVP
Esfenvalerate	0.5	12	0.25	38	CVP
Ethofumesate	No effect		1	10	CVP, PE
Fenpyroximate (Z,E)	No effect		0.25	90	ISV
Flumetralin	No effect		No effect		CVP
Indoxacarb	20	12	10	38	CVP
Lactofen	No effect		No effect		PE
Malaoxon	No effect		0.5	20	CVP
Methomyl	10		1	15	CVP
Niclosamide	No effect		0.5	11	ISV
Oryzalin	0.1	28	10	28	CVP
Pendimethalin	1	10	1	40	CVP
Pyraclostrobin	0.35	89	0.25	11	ISV, CVP

Chemical name	LEL for ISV perturbations (μM)	Embryos with perturbed ISVs at LEL (%)	LEL for CVP perturbations (μM)	Embryos with perturbed CVP at LEL (%)	Effect by visual determination
Pyridaben	0.1	11	0.25	40	ISV
Quinoxyfen	No effect		No effect		CVP
Resmethrin	10	20	0.25	29	CVP
Rotenone	0.025	33	0.02	33	ISV, CVP
Tebufenpyrad	0.5	90	0.25	23	CVP
Tebupirimfos	10	20	20	25	ISV, CVP, BC
Tetramethrin	0.5	14	0.5	14	PE
Thiodicarb	10	17	10	67	CVP, PE
Tribufos	1	14	0.1	27	CVP
Trifloxystrobin	0.25	17	0.35	42	ISV, CVP

* Compounds with “No effect” were initially found to cause vascular disruption via visual assessment, but not via automated image analysis.

PE=Pericardial edema; BC=Blood clot, accumulation or hemorrhage; CVP=Caudal vein plexus phenotype; ISV=Intersegmental vessel phenotype; DA=Dorsal aorta; PCV=Posterior cardinal vein